

Review

# Protein–lipid interactions in the purple bacterial reaction centre

Michael R. Jones<sup>a,\*</sup>, Paul K. Fyfe<sup>a</sup>, Aleksander W. Roszak<sup>b</sup>,  
Neil W. Isaacs<sup>b</sup>, Richard J. Cogdell<sup>c</sup>

<sup>a</sup>Department of Biochemistry, School of Medical Sciences, University of Bristol, University Walk, Bristol, BS8 1TD, UK

<sup>b</sup>Department of Chemistry, University of Glasgow, Glasgow, G12 8QQ, UK

<sup>c</sup>Division of Biochemistry and Molecular Biology, University of Glasgow, Glasgow, G12 8QQ, UK

Received 6 February 2002; received in revised form 10 June 2002; accepted 10 June 2002

## Abstract

The purple bacterial reaction centre uses the energy of sunlight to power energy-requiring reactions such as the synthesis of ATP. During the last 20 years, a combination of X-ray crystallography, spectroscopy and mutagenesis has provided a detailed insight into the mechanism of light energy transduction in the bacterial reaction centre. In recent years, structural techniques including X-ray crystallography and neutron scattering have also been used to examine the environment of the reaction centre. This mini-review focuses on recent studies of the surface of the reaction centre, and briefly discusses the importance of the specific protein–lipid interactions that have been resolved for integral membrane proteins.

© 2002 Elsevier Science B.V. All rights reserved.

**Keywords:** Reaction centre; Photosynthesis; X-ray crystallography; Mutagenesis; Water; Ubiquinone; Cardiolipin

## 1. Introduction

The bacterial reaction centre was the first integral membrane protein to yield a high-resolution X-ray crystal structure. In the mid-1980s, structures were determined for the reaction centres from *Rhodospseudomonas (Rps.) viridis*<sup>1</sup> and *Rhodobacter (Rb.) sphaeroides*, and subsequently there has been a gradual improvement in the resolution and quality of the structures of the wild-type proteins (see Ref. [1] for a recent review of this). In addition to being used as a model system for examining the principles of light energy transduction in photosynthesis, the bacterial reaction centre has also played an important role in the study of general principles of membrane protein design, protein dynamics and biological electron transfer. In recent years, crystallo-

graphic studies of the bacterial reaction centre have provided new structural information related to the function of the complex, and on the structural consequences of mutagenesis (see for review Refs. [1,2]).

This mini-review looks at investigations of the immediate surface environment of the bacterial reaction centre, a facet of structural studies of the complex that has only very recently been developed. New advances in this area are discussed, and comparisons are made with related findings for other integral membrane proteins.

## 2. The structure and mechanism of the bacterial reaction centre

Fig. 1 outlines the structure and mechanism of the bacterial reaction centre, using the complex from *Rb. sphaeroides* as example. The architectures of the *Rps. viridis* and *Rb. sphaeroides* reaction centres are constructed on a common principle, and the similarities and differences between them have been extensively discussed [3,4].

Fig. 1A shows the overall structure of the *Rb. sphaeroides* reaction centre, and Fig. 1B shows the arrangement of the reaction centre cofactors. The 10 cofactors are encased by two protein subunits (L and M) that each has five trans-

*Abbreviations:* BChl, bacteriochlorophyll; BPhe, bacteriopheophytin; P, primary donor of electrons; PDB, Protein Data Bank; *Rb.*, *Rhodobacter*; *Rps.*, *Rhodospseudomonas*

\* Corresponding author. Tel.: +44-117-9287571; fax: +44-117-9288274.

*E-mail address:* m.r.jones@bristol.ac.uk (M.R. Jones).

<sup>1</sup> It has been proposed that *Rhodospseudomonas viridis* should be renamed *Blastochloris viridis* [63]. As the former name has permeated the literature on the bacterial reaction centre for almost 20 years, and it is still in widespread use, it will be used throughout this article.

membrane  $\alpha$ -helices (Fig. 1A). The L- and M-subunits are arranged around an axis of pseudo twofold symmetry that is orientated perpendicular to the plane of the membrane. A third subunit, named H, caps the cytoplasmic faces of the L- and M-subunits and has a single trans-membrane  $\alpha$ -helix

(Fig. 1A). The BChl, BPhe and ubiquinone cofactors are arranged in two membrane-spanning branches, also around the axis of pseudo twofold symmetry (Fig. 1B). The reaction centre catalyses an energetically uphill reaction, the reduction of ubiquinone by cytochrome  $c_2$ , and to achieve this, light energy is used to initiate the electron transfer process. Many reviews have been published that provide detailed descriptions of the mechanism of light-driven electron transfer in the reaction centre and spectroscopy of the complex (for examples see Refs. [5–10]).

In terms of design, the reaction centre shows the classic features of an alpha-helical membrane-spanning protein. A surface potential map (Fig. 1C) shows that most of the protein that is exposed on either side of the membrane is coated with hydrophilic residues, which show up as regions of positive (blue) or negative (red) potential [11]. In marked contrast, the intra-membrane surface of the protein is distinguished by wide band of neutral surface potential (Fig. 1C). The protein in this region consists of a bundle of 11 tightly packed membrane-spanning  $\alpha$ -helices that have hydrophobic residues on the helix surfaces that are exposed to the membrane interior. When the protein is purified, this hydrophobic surface is shielded from the aqueous phase by the detergent micelle, and neutron diffraction experiments have shown the structure of this micelle in crystals of the reaction centre [12,13].

### 3. The complex environment of the bacterial reaction centre

In the native membrane, the bacterial reaction centre undergoes interactions with a range of molecules in its environment. On either side of the membrane, the cytoplasmic and periplasmic faces of the protein interact with molecules in the adjacent aqueous environments. The most obvious of these is the transient interaction that takes place on the periplasmic side of the membrane with cytochrome  $c_2$ ,

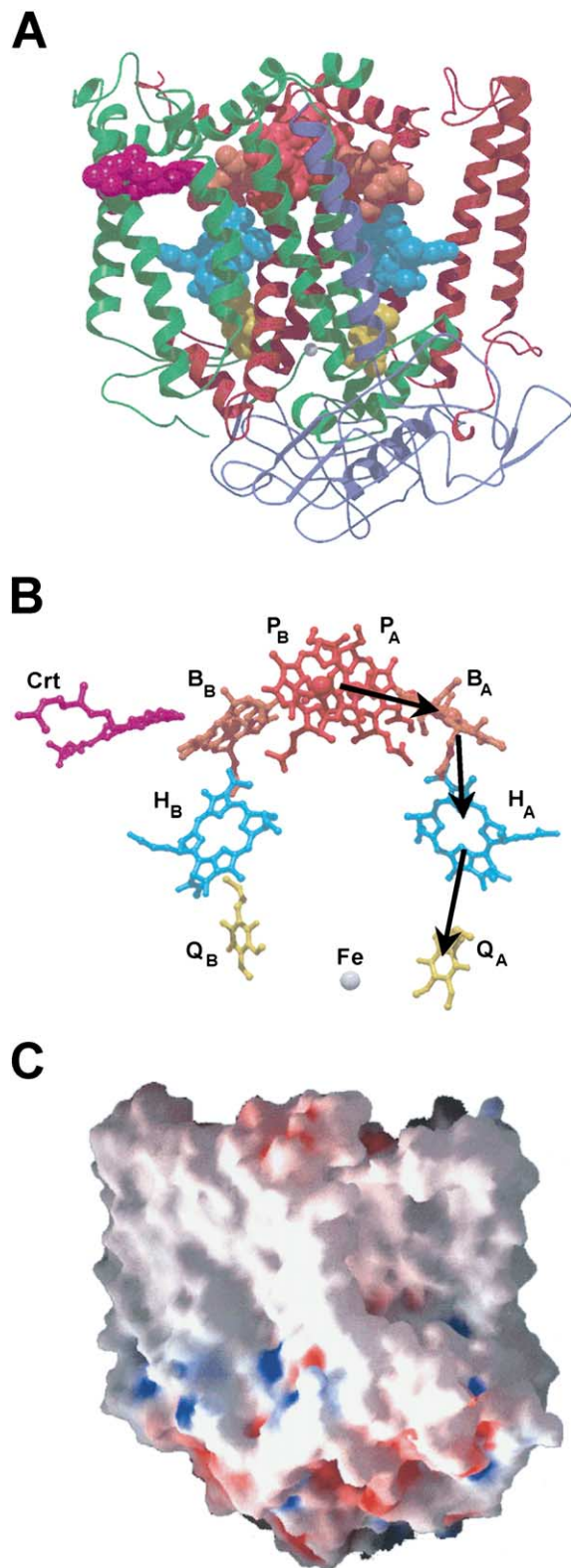


Fig. 1. Overview of the structure of the *Rb. sphaeroides* reaction centre. (A) Shows the overall structure of the complex. The L-, M- and H-subunits are shown as maroon, green and purple ribbons, respectively. These encase 10 cofactors, shown as connected spheres. These are a dimer of bacteriochlorophyll (red), two accessory bacteriochlorophylls (sienna), two bacteriopheophytins (cyan), two ubiquinones (yellow), a spheroidenone carotenoid (pink) and a non-heme iron atom (grey). The isoprenoid side chains of the bacteriochlorophyll, bacteriopheophytin and ubiquinone cofactors have been omitted for clarity. (B) Shows the arrangement of the reaction centre cofactors, shown in stick format. The symmetry axis runs from the pair of bacteriochlorophylls on one side of the membrane (P<sub>A</sub> and P<sub>B</sub>—red) to the non-heme iron on the opposite side of the membrane (Fe—grey sphere). The accessory bacteriochlorophylls (B<sub>A</sub> and B<sub>B</sub>—sienna), bacteriopheophytins (H<sub>A</sub> and H<sub>B</sub>—cyan) and ubiquinones (Q<sub>A</sub> and Q<sub>B</sub>—yellow) are arranged in two membrane-spanning branches. Only the A-branch is active in transmembrane electron transfer, indicated by the arrows. (C) View of the reaction centre as a solid object, with the surface coloured according to surface potential (blue—positive; red—negative; white—neutral). The figure was prepared using the programs Molscript [64], Raster3D [65] and GRASP [66].

the electron donor to the photo-oxidised reaction centre. The reaction centre and cytochrome  $c_2$  from *Rb. sphaeroides* have been successfully co-crystallised, and the structure of the resulting complex has been described to a resolution of  $\sim 4.5 \text{ \AA}$  [14]. In the co-crystals the cytochrome makes contacts with both the L- and M-subunits at the periplasmic surface of the reaction centre, although these contacts have not been described in fine detail. The rate of electron transfer from cytochrome  $c_2$  to the reaction centre was determined in the co-crystal and was found to be the same as that between these proteins in solution [14]. This showed that the modelled orientation of the cytochrome with respect to the reaction centre in the crystal could be the same as that adopted by the proteins in vivo, but did not prove this to be the case.

In recent studies, a binding site for  $\text{Zn}^{2+}$  (or  $\text{Cd}^{2+}$ ) on the cytoplasmic surface of the reaction centre has been identified by X-ray crystallography [15]. This work was prompted by the observation that the rate of electron transfer [16] and proton transfer [17] to the  $\text{Q}_B$  ubiquinone reductase site on the cytoplasmic side of the membrane is reduced by stoichiometric binding of  $\text{Zn}^{2+}$  to the *Rb. sphaeroides* reaction centre. The binding site for these divalent cations involves two His and one Asp residue at the cytoplasmic surface of the H-subunit [15]. The Asp residue (H124) forms the end of a short hydrogen bond network that connects the surface of the protein with the  $\text{Q}_B$  binding site. This network involves three water molecules and residues Ser L223, Asp L213, Asp M17 and Asp L210 [18]. Recently, it has been demonstrated that  $\text{Cu}^{2+}$  has a similar effect to  $\text{Zn}^{2+}$  on the rate of electron transfer from the  $\text{Q}_A$  to  $\text{Q}_B$  ubiquinone, and it has been proposed the reaction centre has a discrete  $\text{Cu}^{2+}$  binding site [19]. This involves four His residues that are located at the cytoplasmic surface of the protein, in a region of close contact between the H-, L- and M-subunits [19].

Turning to the intra-membrane surface of the protein, the expectation is that the environment of the reaction centre will consist of a mixture of lipids and other integral membrane proteins. Interactions with membrane lipids are considered in the next section. In the case of protein–protein interactions, it is known that the reaction centre interacts with another integral membrane protein, the LH1 antenna complex, to form the so-called RC/LH1 core complex. The pigments of the LH1 antenna, bacteriochlorophyll and carotenoid, harvest light energy and transmit the energy to the reaction centre, where photochemistry initiates trans-membrane electron transfer.

A general view of the structure of the RC/LH1 core complex has emerged through a combination of relatively low-resolution electron diffraction images of LH1 antenna [20,21], and structural homologies with the LH2 antenna complex (where high-resolution X-ray crystal structures are available [22,23]). The LH1 antenna is thought to form a cylinder of protein and pigment that surrounds the reaction centre in the membrane, with the bacteriochlorophylls of the reaction centre and LH1 antenna present at a fixed stoichi-

ometry. A number of groups have produced theoretical models of the structure of the antenna/reaction centre system in purple bacteria [24–28], and most of these show the reaction centre surrounded by a closed cylinder of LH1 antenna complex. However, there are some questions as to whether this cylinder is complete in vivo, at least in some species [29]. In *Rb. sphaeroides* the RC/LH1 core complex also contains one or two copies of a membrane protein called PufX, which is thought to disrupt the continuity of the cylinder of LH1 pigment–protein complex surrounding the reaction centre [28]. As yet, there is no detailed molecular information on protein–protein contacts between the reaction centre and the LH1 antenna complex, or the structural role played by the PufX protein.

#### 4. The lipid environment of the bacterial reaction centre

In addition to molecular interactions with adjacent proteins, integral membrane proteins also interact with the lipids of the membrane. As discussed in a recent review [11], EPR spectroscopy suggests that a protein of the size and shape of the bacterial reaction centre will be surrounded by a shell of between 30 and 35 “annular” lipids that are motionally restricted as a result of their interaction with the protein surface [30]. The fact that these lipids are motionally restricted raises the possibility that they can be detected through X-ray crystallography, provided that the lipid is not displaced from the protein surface during detergent purification. In addition, it is necessary that the restriction in motion extends to a sufficient fraction of the lipid molecule, so that it is sufficiently well-ordered to be seen in X-ray diffraction.

When the reaction centre is purified, molecular interactions with the membrane lipids are replaced by reaction centre-detergent interactions. The structures of the detergent micelle in crystals of the *Rps. viridis* and *Rb. sphaeroides* reaction centre have been visualised by neutron diffraction [12,13], and it has been found that the detergent forms an ellipsoid micelle around the membrane-spanning hydrophobic surfaces of the reaction centre, mimicking the expected lipid environment of the native complex.

Many of the structural models for the bacterial reaction centre deposited in the Protein Data Base include molecules of the detergent lauryl dimethylamineoxide (LDAO) fitted into the electron density [1]. With all but one exception, these detergent molecules are modelled as interacting with the hydrophobic intra-membrane surface of the reaction centre. In Fig. 2, we show examples of the sort of electron density features that can be observed at the surface of the reaction centre, but which cannot be attributed to the reaction centre protein or cofactors. Our own studies with different mutant *Rb. sphaeroides* reaction centres have shown that the number and extent of these elongated “sausages” of electron density varies considerably between different X-ray structures (unpublished data). These differences could be due to

variability in different reaction center preparations, or to the variable data quality of the different structural determinations.

### 5. Specific reaction centre–lipid interactions—cardiolipin

One structural model of the *Rb. sphaeroides* reaction centre in the Protein Data Bank, deposited by us, includes a molecule of the anionic lipid diphosphatidyl glycerol, or cardiolipin [31]. The modelled lipid is located on the intramembrane surface of the protein, on the cytoplasmic side of the membrane and close to the trans-membrane  $\alpha$ -helix of the H-subunit. Cardiolipin is a diacidic lipid, consisting of a polar head group that is composed of three glycerol molecules connected by two phosphodiester linkages, and four hydrophobic acyl chains. The head group and adjacent parts of the ends of the acyl chains were clearly resolved in the electron density map, which was that of a mutant *Rb. sphaeroides* reaction centre (Ala M260 to Trp; AM260W) at a resolution of 2.1 Å [31]. The ends of the acyl chains were not resolved, presumably because they were mobile and therefore disordered, and so were modelled as chains of between 9 and 15 carbons in length. Double bonds were not included in the models of the acyl tails, as their presence and/or exact position could not be determined from the electron density with sufficient certainty. This cardiolipin is also included in a number of structures for mutant *Rb. sphaeroides* reaction centres deposited recently in the Protein Data Bank by Camara-Artigas et al. [32].

On detailed examination of the structural model, several possible bonding interactions were observed between the phosphates of the lipid head-group and the surrounding protein [31]. Three direct contacts were observed, involving the side chains of residues Arg M267 and His M145, and the backbone amide of Lys M144. The cardiolipin also made indirect contacts to Lys M144, Arg M267, Tyr H30, Trp M146 and Trp M271 via four crystallographically defined water molecules. The acyl chains of the cardiolipin traced along hydrophobic grooves in the intra-membrane surface of the protein, and depicted very nicely how interactions with

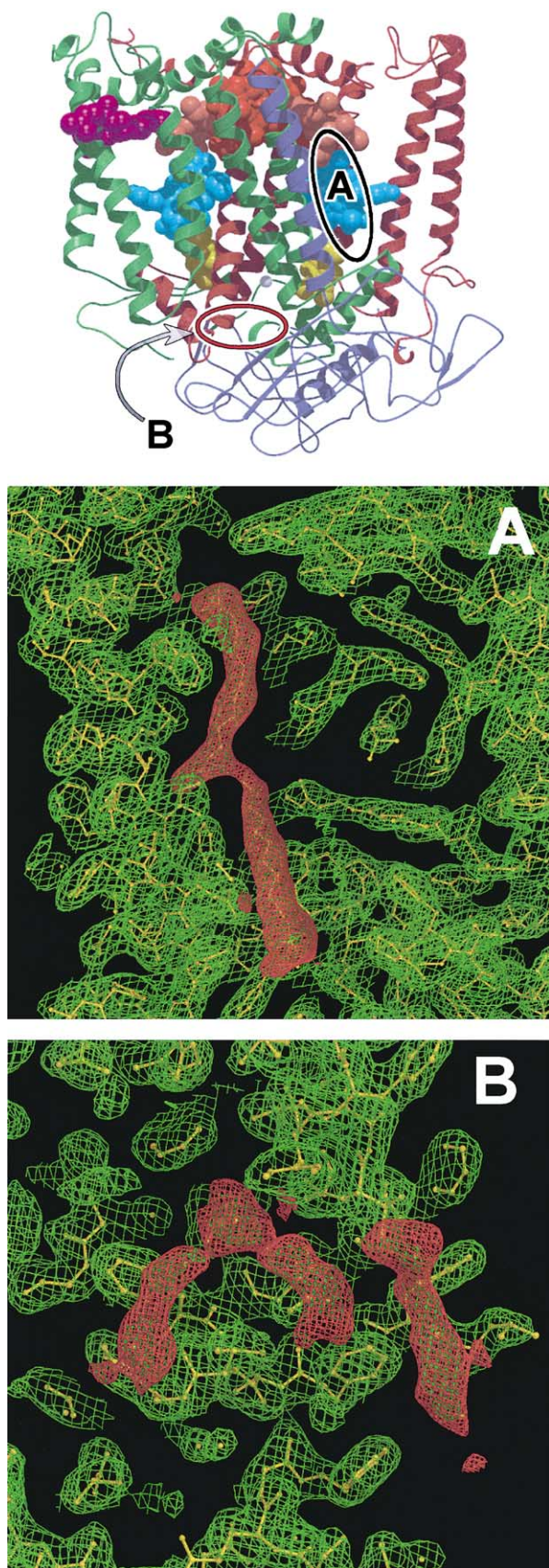


Fig. 2. Unattributed electron density features at the surface of the *Rb. sphaeroides* reaction centre (FM197R/GM203D mutant [69]). The top panel shows the structure of the *Rb. sphaeroides* reaction centre, coloured as in Fig. 1, with two regions highlighted. The lower panels show REFMAC 2mF<sub>o</sub>-DF<sub>c</sub> maps (green) of all of the electron density with the fitted structure of the protein (yellow sticks). Overlaid is a REFMAC mF<sub>o</sub>-DF<sub>c</sub> map (red) of the unassigned density found in regions A (middle) and B (bottom). Region A is adjacent to the cardiolipin binding site, but on the opposite side of the transmembrane,  $\alpha$ -helix of the H-subunit (purple ribbon, top panel). In the structure of the *Tch. tepidum* reaction centre this region is occupied by a molecule of phosphatidyl ethanolamine (see text). Region B is at the rear of the complex in the view shown in the top panel, on the opposite face of the reaction centre to the cardiolipin binding site. The figure was prepared using the programs Molscript [64], Raster3D [65] and XtalView [67].

the irregular protein surface will bring about a restriction in the motional freedom of adjacent lipids.

Although it has been established that bacteriochlorophyll-containing proteins from purple bacteria preferentially associate with negatively charged lipids, including cardiolipin [33,34], there has been no study of the relevance of cardiolipin to the structural and functional integrity of the bacterial reaction centre. An interesting point is that the residues that bind the head-group of the cardiolipin are strongly conserved across a wide range of purple photosynthetic bacteria [35], which provides circumstantial evidence that this protein–lipid interaction is a conserved feature of the complex.

The first report of a molecule of cardiolipin bound to the intra-membrane surface of the *Rb. sphaeroides* reaction centre [31] was published more than 10 years after the first descriptions of the high-resolution structure of this complex, and that of the related *Rps. viridis* reaction centre [36–40]. As discussed in detail elsewhere, in studies by a number of groups (including our own), electron density on the surface of the protein in this region occupied by cardiolipin in the structure of the AM260W mutant has been variously mod-

elled as a molecule of phosphate or sulfate, and/or one or more molecules of the detergent LDAO [31].

In Fig. 3, we show the relevant region of the electron density maps for the wild-type *Rb. sphaeroides* reaction centre and five mutant complexes. The data in Fig. 3A–F are shown in order of the clarity with which the electron density feature attributed to cardiolipin is resolved. In Table 1 we show statistics to indicate the relative quality of the data that gave rise to these maps, the data collection conditions used, as well as indicator statistics from the refinements. The electron density maps clearly show the variability in the extent and completeness of the electron density feature from data set to data set (Fig. 3). The structure in which the cardiolipin is most clearly resolved (mutant AM260W; Fig. 3A) is the best in terms of the quality of the original data, as assessed by the high resolution cut-off, R-factors and multiplicity of the data. However, the two “next best” structures, in which the electron density feature is resolved to similar extents, are derived from data of differing quality. The data set for the WM115F/FM197R reaction centre (Fig. 3C) is of relatively high quality, whereas the data set for the GM203D/FM197R mutant (Fig. 3B) is the lowest quality of the six

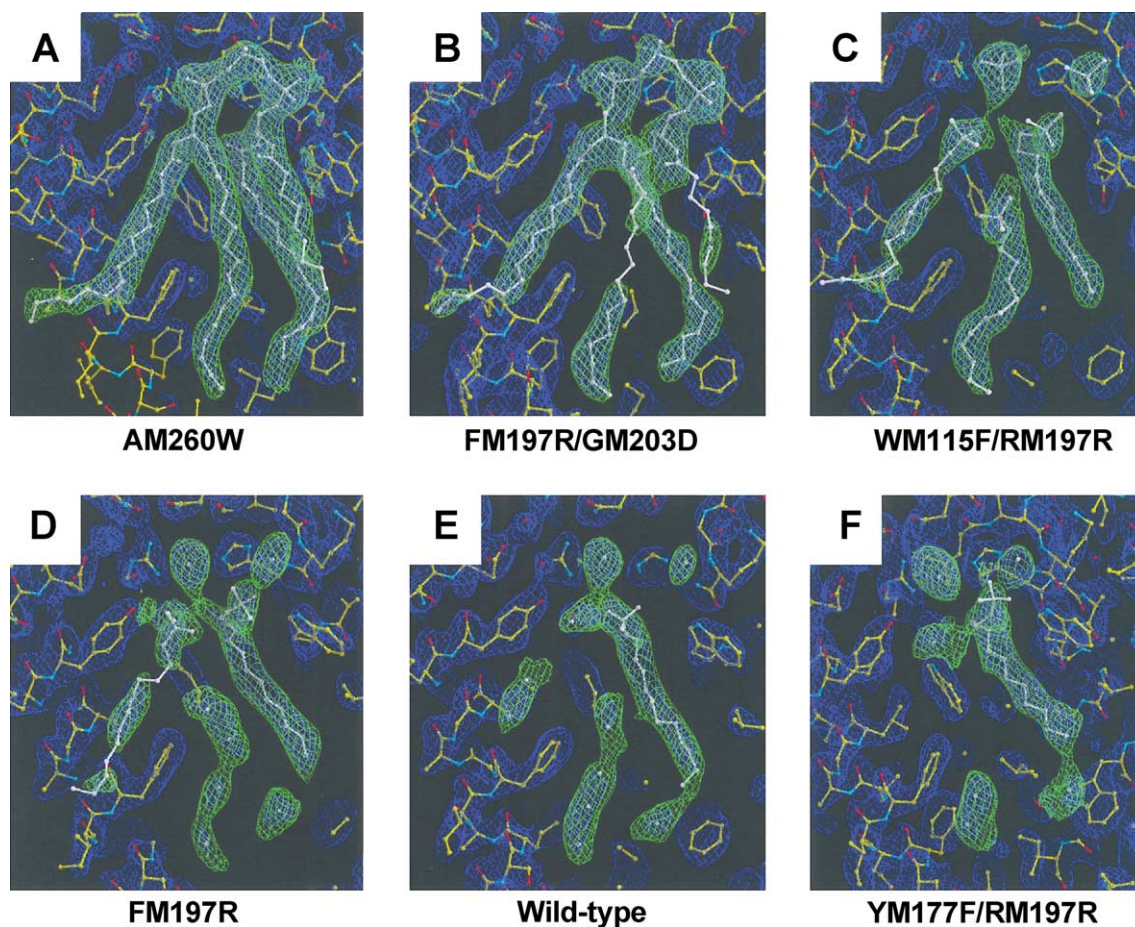


Fig. 3. The site of cardiolipin binding on the intramembrane surface of six *Rb. sphaeroides* reaction centres that have been characterised by X-ray crystallography. In each case, we show a REFMAC  $2mF_o - DF_c$  map (blue) of the electron density attributed to the entire structure, with the fitted structure of the protein (cpk colours). The electron density that is not attributable to the protein is highlighted in green. The sources of the data used are given in Table 1. The figure was prepared using the programs Raster3D [65] and XtalView [67].

Table 1  
Crystallographic statistics for structures of the wild-type *Rb. sphaeroides* reaction centre, and five complexes with mutations in the M-subunit<sup>a</sup>

Parameter	AM260W	FM197R/GM203D	WM115F/FM197R	FM197R	Wild-type	YM177F/FM197R
Resolution range (Å)	30–2.1	30–2.7	26.4–2.3	16.5–2.55	11–2.6	11–2.55
Number of reflections	124,853	53,587	90,855	67,571	64,071	54,163
Multiplicity	4.1	2.8	3.8	not available	2.6	3.0
R-factor (%)	16.9	22.6	17.4	20.2	18.3	19.4
Free R-factor (%)	18.6	26.8	20.0	22.2	20.4	21.7
Number of crystals used	2	1	7	not available	1	2
Data collection temperature (K)	298	100	298	298	298	298
Precipitant	trisodium citrate	potassium phosphate	potassium phosphate	potassium phosphate	potassium phosphate	potassium phosphate
PDB code	1QOV	1E14	1E6D	–	–	1MPS

<sup>a</sup> Data is taken from: AM260W [68], FM197R/GM203D [69], WM115F/FM197R [70], FM197R [71], wild-type [70,72], YM177F/FM197R [70,72]. Each structure includes one molecule of cardiolipin.

presented. The only possible correlation that can be made is that the three structures in which the electron density feature was most complete (Fig. 3A–C) included low resolution data in the 20.0 to 30.0 Å range.

The other possibility we have considered for the variation in the completeness of the electron density feature shown in Fig. 3 is that it is a reflection of the occupancy of this site by cardiolipin. Once again, we have not been able to identify an obvious cause for such variation. All of the reaction centres used in the work summarized in Fig. 3 were prepared from antenna-deficient intracytoplasmic membranes that, in turn, had been prepared from bacterial cells grown under semi-aerobic conditions in the dark. The reaction centres were isolated by solubilisation of the antenna-deficient membranes using LDAO, and purified by column chromatography, using essentially the same protocol in each case. The one exception to this is that trisodium citrate was used as the precipitant for crystallisation of the AM260W reaction centre, where the cardiolipin was most clearly resolved (Fig. 3A), rather than the potassium phosphate used in the remaining studies. However, we feel that it is unlikely that this is a significant factor, as cardiolipin density of a quality similar to that shown for the AM260W mutant in Fig. 3a was obtained for a YM210W mutant reaction centre described recently [41], and in a number of new unpublished structures. In all of these cases, the precipitant used was potassium phosphate.

## 6. Specific reaction centre–lipid interactions—phosphatidyl ethanolamine in *Thermochromatium tepidum*

Recently, a high-resolution (2.2 Å) X-ray crystal structure has been described for the reaction centre from *Tch. tepidum* [42,43]. This is a moderately thermophilic purple sulfur bacterium isolated from the hot springs of the Yellowstone National Park [44], and was formerly known as *Chromatium tepidum* [45]. *Tch. tepidum* has an optimum growth temperature of between 48 and 50 °C, and will tolerate temper-

atures up to 58 °C [44,46]. The *Tch. tepidum* reaction center shows an enhanced thermal stability in both intact membranes and detergent-micelles [47]. Accompanying the description of the X-ray structure of this reaction centre were discussions by Nogi et al. [42] and Fathir et al. [43] of aspects of the structure that might contribute to this enhanced thermal stability.

In terms of overall architecture, the *Tch. tepidum* reaction centre is similar to the *Rps. viridis* complex in that it contains a fourth subunit comprising a tetra-heme cytochrome that is attached to the periplasmic face of the L- and M-subunits. In addition to the protein and cofactors, the structural model of the *Tch. tepidum* reaction centre included seven molecules of the detergent  $\beta$ -octylglucoside and one molecule of LDAO [42,43]. The cardiolipin included in models of the *Rb. sphaeroides* reaction centre was not detected in the structure of the *Tch. tepidum* complex, but one of the molecules of  $\beta$ -octylglucoside was modelled in a position that corresponds to acyl chain 1 of cardiolipin in the *Rb. sphaeroides* reaction centre [42]. This acyl chain makes extensive contacts with the trans-membrane  $\alpha$ -helix of the H-subunit [31,35].

It is worth pointing out that the residues that engage in bonding interactions with the head-group of cardiolipin in the *Rb. sphaeroides* reaction centre are conserved in the *Tch. tepidum* complex, including the main bonding residues Arg M267 and His M145. To our knowledge there is no data on the lipid composition of the *Tch. tepidum* cytoplasmic membrane, but cardiolipin has been reported to be a major component of the membrane from three other species of Chromatiaceae [48], namely *Chromatium vinosum* (now *Allochromatium vinosum* [45]), *Chromatium minus* (now *Thiocystis minor* [45]) and *Thiocystis gelatinosa*. In the light of this, and the widespread occurrence of this lipid in other types of photosynthetic prokaryotes [48], it seems possible that cardiolipin is present in the photosynthetic membrane of *Tch. tepidum*.

Although the structural model of the *Tch. tepidum* reaction centre did not contain a modelled cardiolipin, it did include a molecule that was assigned as dipalmitoyl-3-*sn*-

phosphatidyl ethanolamine (PE), with two saturated 16-carbon acyl chains [42,43]. This lipid was also located adjacent to the cytoplasmic half of the trans-membrane  $\alpha$ -helix of the H-subunit, but on the opposite side of the helix to the site occupied by cardiolipin in the *Rb. sphaeroides* complex. The PE occupies a deep groove in the protein surface formed by the H-subunit trans-membrane  $\alpha$ -helix and the trans-membrane  $\alpha$ -helices of the L- and M-subunits, and the phosphate of the head-group of the lipid is bound to residues Arg H31 and Lys H35. Interestingly, as discussed by Fathir et al. [43], these basic residues are not conserved in the *Rb. sphaeroides* reaction centre, where they are Gln and Met, respectively. As shown in Fig. 4, these substitutions significantly change the potential of the protein surface in the region adjacent to the head-group of the PE. In *Tch. tepidum* (Fig. 4, left), the Arg and Lys create a region of positive potential that interacts with the head group of the PE, whereas in *Rb. sphaeroides* (Fig. 4, right), a theoretical model of the PE superimposed on the reaction centre shows that this area of the protein is largely electroneutral. In our crystallographic studies of the *Rb. sphaeroides* reaction centre we have not observed any electron density in a position equivalent to the head-group of the PE. However, in some data sets we have observed an elongated density feature approximately in the position of the tail of the PE that is closest to the trans-membrane  $\alpha$ -helix of the H-subunit. This feature is shown in the middle panel of Fig. 2.

In their recent report [43], Fathir and co-workers pointed out that in the 3PRC structural model of the *Rps. viridis* reaction center [49], where Arg H31 and Lys H35 are both Arg residues (H33 and H37, respectively), density features in this region of the protein have been modelled as a sulfate ion and two molecules of LDAO. The positions of these correspond to the head-group phosphate and the acyl chains of the PE in the structural model of the *Tch. tepidum* reaction centre, suggesting that the density seen in the data on the

*Rps. viridis* complex could be incomplete density that actually corresponds to a lipid such as phosphatidyl ethanolamine [43]. This draws interesting parallels to the data on cardiolipin binding by the *Rb. sphaeroides* reaction centre outlined in Fig. 3, and described above.

Finally, Nogi et al. [42] have also discussed the possible structural origins of the enhanced thermal stability exhibited by the *Tch. tepidum* reaction centre. The feature highlighted by the structure and by sequence comparisons was the presence of three arginine residues on the surface of the L- and M-subunits that are not present in reaction centres from mesophilic bacteria. These arginines, at positions L71, L84 and M104, are a suitable position to interact with the head-groups of lipids on the periplasmic side of the membrane, and Nogi and coworkers speculated that the enhanced thermal stability of the *Tch. tepidum* reaction centre is contributed to by a stronger interaction with the surrounding membrane lipids [42].

## 7. Lipids in X-ray crystal structures of integral membrane proteins

A number of structures for other integral membrane proteins, obtained by either X-ray or electron diffraction, have included bound lipids or lipopolysaccharides in the published structural model [11]. These include structures for bacteriorhodopsin with as many as 18 archaeal lipids [50–55], cytochrome *c* oxidase with up to 14 lipids (phosphatidyl ethanolamine, phosphatidyl choline and phosphatidyl glycerol) [56–58], the ferric hydroxamate uptake receptor (FhuA) from *Escherichia* (*E. coli*) with a bound lipopolysaccharide [59], and formate dehydrogenase–N from *E. coli* with a bound cardiolipin [60].

Very recently, the groups of Witt and Saenger in Berlin have published an X-ray crystal structure, at 2.5-Å resolu-

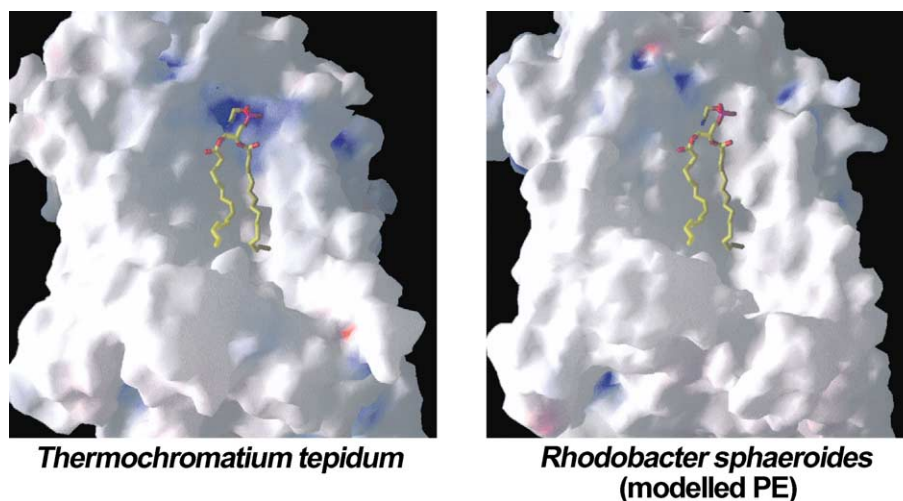


Fig. 4. Surface representation of (left) the *Tch. tepidum* reaction centre with the bound phosphatidyl ethanolamine and (right) the wild-type *Rb. sphaeroides* reaction centre with a phosphatidyl ethanolamine modelled at the analogous position. The protein was coloured according to surface potential (blue—positive; red—negative; white—neutral). The figure was prepared using the program GRASP [66].

tion, of a trimeric form of the Photosystem-I reaction centre isolated from the thermophilic cyanobacterium *Synechococcus elongatus* [61,62]. This structure includes four lipids per monomer, three molecules of phosphatidyl glycerol and one molecule of monogalactosyldiglyceride [62]. In an intriguing development, the phosphodiester group of one of the phosphatidyl glycerol molecules is observed to provide the axial ligand to the central magnesium atom of one of the Photosystem-I chlorophyll cofactors. This phosphatidyl glycerol is located on the surface of the PsaA protein, a major component of each monomer, at the interface between monomers in the Photosystem-I trimer [61,62].

Following from this last point, a feature of many of the lipids that have been resolved is that they are bound at the interface between monomers in a multimeric structure [50,52–55,57,60,62]. This points towards a significant role of membrane lipids in forming much of the contact surface between closely associated proteins in the membrane, in addition to their roles in forming a “sea of lipid” surrounding protein structures. In both cytochrome *c* oxidase and the Photosystem-I reaction centre, lipids also form part of the contact surface between polypeptide chains within a monomer [57,62]. Of course when located at these interface positions these lipids are likely to be strongly motionally restricted, and so can be more readily detected by X-ray crystallography.

## 8. Conclusions and outlook

As more high resolution structures of membrane proteins appear, we can expect to “see” more examples of lipid–protein interactions. When these become available, it will be important to examine whether there are distinct classes of these interactions, both with regard to the types of lipid and the functions they may have, and to discover whether any general principles can be established. One of the difficulties in this type of study is the problem of discriminating electron density due to lipids that remain attached to the purified protein from that arising from bound detergent molecules. One possible way to overcome this problem is to crystallise membrane proteins in the presence of either detergents or lipids that have been labelled with strongly diffracting atoms such as bromine. We are currently exploring this approach with crystals of the *Rb. sphaeroides* reaction centre.

## 9. Note added in proof

Whilst this article was in press two papers were published that are highly relevant to the content of this mini-review. Axelrod and co-workers [73] have reported a new X-ray crystal structure at 2.4 Å resolution for a functional co-complex formed between the *Rb. sphaeroides* reaction centre at cytochrome *c*<sub>2</sub>, that places the cytochrome at the centre of the periplasmic face of the reaction centre.

Camara-Artigas and co-workers [74] have reported a new X-ray crystal structure of the wild-type *Rb. sphaeroides* reaction centre that contains two modelled lipids in addition to the cardiolipin discussed in this article. These additional lipids, a glucosylgalactosyl diacylglycerol and a phosphatidylcholine, are modelled into more extensive versions of the electron density features shown in panels A and B, respectively, of Figure 2 of this review. The structure of Camara-Artigas and co-workers was based on diffraction data collected over the resolution range 30.0–2.55 Å, and so included the low resolution terms.

## Acknowledgements

The authors wish to thank the BBSRC and the Wellcome Trust for financial support.

## References

- [1] P.K. Fyfe, M.R. Jones, *Biochim. Biophys. Acta* 1459 (2000) 413–421.
- [2] P.K. Fyfe, K.E. McAuley-Hecht, M.R. Jones, R.J. Cogdell, in: P.I. Haris, D. Chapman (Eds.), *Biomembrane Structures*, IOS Press, Amsterdam, The Netherlands, 1998, pp. 64–87.
- [3] J.P. Allen, G. Feher, T.O. Yeates, D.C. Rees, J. Deisenhofer, H. Michel, R. Huber, *Proc. Natl. Acad. Sci. U. S. A.* 83 (1986) 8589–8593.
- [4] O. El Kabbani, C.H. Chang, D. Tiede, J. Norris, M. Schiffer, *Biochemistry* 30 (1991) 5361–5369.
- [5] W.W. Parson, in: H. Scheer (Ed.), *Chlorophylls*, CRC Press, Boca Raton, FL, USA, 1991, pp. 1153–1180.
- [6] G.R. Fleming, R. van Grondelle, *Phys. Today* 47 (1994) 48–55.
- [7] N.W. Woodbury, J.P. Allen, in: R.E. Blankenship, M.T. Madigan, C. Bauer (Eds.), *Anoxygenic Photosynthetic Bacteria*, Kluwer Academic Publishing, The Netherlands, 1995, pp. 527–557.
- [8] W.W. Parson, in: D.S. Bendall (Ed.), *Protein Electron Transfer*, BIOS Scientific Publishers, Oxford, UK, 1996, pp. 125–160.
- [9] A.J. Hoff, J. Deisenhofer, *Phys. Lett.* 287 (1997) 2–247.
- [10] M.E. van Brederode, M.R. Jones, in: N.S. Scrutton, A. Holzenburg (Eds.), *Enzyme-Catalysed Electron and Radical Transfer*, Kluwer Academic Publishing/Plenum, New York, USA, 2000, pp. 621–676.
- [11] P.K. Fyfe, K.E. McAuley, A.W. Roszak, N.W. Isaacs, R.J. Cogdell, M.R. Jones, *Trends Biochem. Sci.* 26 (2001) 106–112.
- [12] M. Roth, A. Lewit-Bentley, H. Michel, J. Deisenhofer, R. Huber, D. Oesterhelt, *Nature* 340 (1989) 659–662.
- [13] M. Roth, B. Arnoux, A. Ducruix, F. Reiss-Husson, *Biochemistry* 30 (1991) 9403–9413.
- [14] N. Adir, H.L. Axelrod, P. Beroza, R.A. Isaacson, S.H. Rongey, M.Y. Okamura, G. Feher, *Biochemistry* 35 (1996) 2535–2547.
- [15] H.L. Axelrod, E.C. Abresch, M.L. Paddock, G. Feher, M.Y. Okamura, *Proc. Natl. Acad. Sci. U. S. A.* 97 (2000) 1542–1547.
- [16] L.M. Utschig, Y. Ohigashi, M.C. Thurnauer, D.M. Tiede, *Biochemistry* 37 (1998) 8278–8281.
- [17] M.L. Paddock, M.S. Graige, G. Feher, M.Y. Okamura, *Proc. Natl. Acad. Sci. U. S. A.* 96 (1999) 6183–6188.
- [18] M.H.B. Stowell, T.M. McPhillips, D.C. Rees, S.M. Soltis, E. Abresch, G. Feher, *Science* 276 (1997) 812–816.
- [19] L.M. Utschig, O. Poluektov, S.L. Schlesselman, M.C. Thurnauer, D.M. Tiede, *Biochemistry* 40 (2001) 6132–6141.
- [20] S. Karrasch, P.A. Bullough, R. Ghosh, *EMBO J.* 14 (1995) 631–638.
- [21] T. Walz, S.J. Jamieson, C.M. Bowers, P.A. Bullough, C.N. Hunter, *J. Mol. Biol.* 282 (1998) 833–845.



- [22] G. McDermott, S.M. Prince, A.A. Freer, A. Hawthornthwaite-Lawless, M.Z. Papiz, R.J. Cogdell, N.W. Isaacs, *Nature* 374 (1995) 517–521.
- [23] J. Koepke, X.C. Hu, C. Muenke, K. Schulten, H. Michel, *Structure* 4 (1996) 581–597.
- [24] M.Z. Papiz, S.M. Prince, A.M. Hawthornthwaite-Lawless, G. McDermott, A.A. Freer, N.W. Isaacs, R.J. Cogdell, *Trends Plant Sci.* 1 (1996) 198–206.
- [25] R.J. Cogdell, P.K. Fyfe, S.J. Barrett, S.M. Prince, A.A. Freer, N.W. Isaacs, P. McGlynn, C.N. Hunter, *Photosynth. Res.* 48 (1996) 55–63.
- [26] X. Hu, K. Schulten, *Biophys. J.* 75 (1998) 683–694.
- [27] X. Hu, A. Damjanović, T. Ritz, K. Schulten, *Proc. Natl. Acad. Sci. U. S. A.* 95 (1998) 5935–5941.
- [28] P.A. Loach, *Proc. Natl. Acad. Sci. U. S. A.* 97 (2000) 5016–5018.
- [29] C. Jungas, J.-L. Ranck, J.-L. Rigaud, P. Joliot, A. Verméglio, *EMBO J.* 18 (1999) 534–542.
- [30] D. Marsh, L.I. Horvath, *Biochim. Biophys. Acta* 376 (1998) 267–296.
- [31] K.E. McAuley, P.K. Fyfe, J.P. Ridge, N.W. Isaacs, R.J. Cogdell, M.R. Jones, *Proc. Natl. Acad. Sci. U. S. A.* 96 (1999) 14706–14711.
- [32] A. Camara-Artigas, C.L. Magee, J.C. Williams, J.P. Allen, *Acta Crystallogr., D* 57 (2001) 1281–1285.
- [33] G.B. Birrell, W.R. Sistrom, O.H. Griffith, *Biochemistry* 17 (1978) 3768–3773.
- [34] W. Welte, W. Kreutz, *Biochim. Biophys. Acta* 692 (1982) 479–488.
- [35] M.C. Wakeham, M.R. Jones, R.B. Sessions, P.K. Fyfe, *Biophys. J.* 80 (2001) 1395–1405.
- [36] J. Deisenhofer, O. Epp, K. Miki, R. Huber, H. Michel, *J. Mol. Biol.* 180 (1984) 385–398.
- [37] J. Deisenhofer, O. Epp, K. Miki, R. Huber, H. Michel, *Nature* 318 (1985) 618–624.
- [38] H. Michel, O. Epp, J. Deisenhofer, *EMBO J.* 5 (1986) 2445–2451.
- [39] J.P. Allen, G. Feher, T.O. Yeates, H. Komiya, D.C. Rees, *Proc. Natl. Acad. Sci. U. S. A.* 84 (1987) 6162–6166.
- [40] H. Komiya, T.O. Yeates, D.C. Rees, J.P. Allen, G. Feher, *Proc. Natl. Acad. Sci. U. S. A.* 85 (1988) 9012–9016.
- [41] K.E. McAuley, P.K. Fyfe, R.J. Cogdell, N.W. Isaacs, M.R. Jones, *FEBS Lett.* 467 (2000) 285–290.
- [42] T. Nogi, I. Fathir, M. Kobayashi, T. Nozawa, K. Miki, *Proc. Natl. Acad. Sci. U. S. A.* 97 (2000) 13561–13566.
- [43] I. Fathir, T. Mori, T. Nogi, M. Kobayashi, K. Miki, T. Nozawa, *Eur. J. Biochem.* 268 (2001) 2652–2657.
- [44] M.T. Madigan, *Science* 225 (1984) 313–315.
- [45] J.F. Imhoff, J. Suling, R. Petri, *Int. J. Syst. Bacteriol.* 48 (1998) 1129–1143.
- [46] M.T. Madigan, *Int. J. Syst. Bacteriol.* 36 (1986) 222–227.
- [47] T. Nozawa, M.T. Madigan, *J. Biochem.* 110 (1991) 588–594.
- [48] J.F. Imhoff, U. Bias-Imhoff, in: R.E. Blankenship, M.T. Madigan, C. Bauer (Eds.), *Anoxygenic Photosynthetic Bacteria*, Kluwer Academic Publishing, The Netherlands, 1995, pp. 179–205.
- [49] C.R.D. Lancaster, H. Michel, *Structure* 5 (1997) 1339–1359.
- [50] N. Grigorieff, T.A. Ceska, K.H. Downing, J.M. Baldwin, R. Henderson, *J. Mol. Biol.* 259 (1996) 393–421.
- [51] K. Mitsuoaka, T. Hirai, K. Murata, A. Miyazawa, A. Kidera, Y. Kimura, Y. Fujiyoshi, *J. Mol. Biol.* 286 (1999) 861–882.
- [52] L.O. Essen, R. Siebert, W.D. Lehmann, D. Oesterhelt, *Proc. Natl. Acad. Sci. U. S. A.* 95 (1998) 11673–11678.
- [53] H. Belrhali, P. Nollert, A. Royant, C. Menzel, J.P. Rosenbusch, E.M. Landau, E. Pebay-Peyroula, *Structure* 7 (1999) 909–917.
- [54] H. Sato, K. Takeda, K. Tani, T. Hino, T. Okada, M. Nakasako, N. Kamiya, T. Kouyama, *Acta Crystallogr., D* 55 (1999) 1251–1256.
- [55] H. Luecke, B. Schobert, H.T. Richter, J.P. Cartailler, J.K. Lanyi, *J. Mol. Biol.* 291 (1999) 899–911.
- [56] T. Tsukihara, H. Aoyama, E. Yamashita, T. Tomizaki, H. Yamaguchi, K. Shinzawa-Itoh, R. Nakashima, R. Yaono, S. Yoshikawa, *Science* 272 (1996) 1136–1144.
- [57] T. Mizushima, et al., *Acta Crystallogr. A55* (Supplement, Abstract P06.04.069).
- [58] A. Harrenga, H. Michel, *J. Biol. Chem.* 274 (1999) 33296–33299.
- [59] A.D. Ferguson, W. Welte, E. Hofmann, B. Lindner, O. Holst, J.W. Coulton, K. Diederichs, *Structure* 8 (2000) 585–592.
- [60] M. Jormakka, S. Tornroth, B. Byrne, S. Iwata, *Science* 295 (2002) 1863–1868.
- [61] P. Jordan, P. Fromme, O. Klukas, H.T. Witt, W. Saenger, N. Krauß, *Nature* 411 (2001) 909–917.
- [62] P. Fromme, P. Jordan, N. Krauß, *Biochim. Biophys. Acta* 1507 (2001) 5–31.
- [63] A. Hiraishi, *Int. J. Syst. Bacteriol.* 47 (1997) 217–219.
- [64] P.J. Kraulis, *J. Appl. Crystallogr.* 24 (1991) 946–950.
- [65] E.A. Merritt, M.E.P. Murphy, *Acta Crystallogr., D* 50 (1994) 869–873.
- [66] A. Nicholls, K.A. Sharp, B. Honig, *Proteins* 11 (1991) 281–296.
- [67] D.E. McRee, *J. Mol. Graph.* 10 (1992) 44–46.
- [68] K.E. McAuley, P.K. Fyfe, J.P. Ridge, R.J. Cogdell, N.W. Isaacs, M.R. Jones, *Biochemistry* 39 (2000) 15032–15043.
- [69] P.K. Fyfe, J.P. Ridge, K.E. McAuley, R.J. Cogdell, N.W. Isaacs, M.R. Jones, *Biochemistry* 39 (2000) 5953–5960.
- [70] P.K. Fyfe, K.E. McAuley-Hecht, J.P. Ridge, S.M. Prince, N.W. Isaacs, R.J. Cogdell, M.R. Jones, *Photosynth. Res.* 55 (1998) 133–140.
- [71] J.P. Ridge, P.K. Fyfe, K.E. McAuley, M.E. van Brederode, B. Robert, R. van Grondelle, N.W. Isaacs, R.J. Cogdell, M.R. Jones, *Biochem. J.* 351 (2000) 567–578.
- [72] K.E. McAuley-Hecht, P.K. Fyfe, J.P. Ridge, S.M. Prince, C.N. Hunter, N.W. Isaacs, R.J. Cogdell, M.R. Jones, *Biochemistry* 37 (1998) 4740–4750.
- [73] A. Camara-Artigas, D. Brune, J.P. Allen, *Proc. Natl. Acad. Sci. U. S. A.* 99 (2002) 11055–11060.
- [74] H.L. Axelrod, E.C. Abresch, M.Y. Okamura, A.P. Yeh, D.C. Rees, G. Feher, *J. Mol. Biol.* 319 (2002) 501–515.